AFRL-RW-EG-TR-2012-092

The Most Accurate Path from Point A to Point B is Not Necessarily a Straight Line

Adam J Rutkowski

Air Force Research Laboratory
Munitions Directorate
101 W Eglin Blvd.
Eglin AFB, FL 32542

20 August 2012

FINAL REPORT

AIR FORCE RESEARCH LABORATORY
MUNITIONS DIRECTORATE

■ **Air Force Materiel Command** ■ **United States Air Force** ■ **Eglin Air Force Base, FL 32542**

NOTICE AND SIGNATURE PAGE

Using Government drawings, specifications, or other data included in this document for any purpose other than Government procurement does not in any way obligate the U.S. Government. The fact that the Government formulated or supplied the drawings, specifications, or other data does not license the holder or any other person or corporation; or convey any rights or permission to manufacture, use, or sell any patented invention that may relate to them.

Qualified requestors may obtain copies of this report from the Defense Technical Information Center (DTIC) <http://www.dtic.mil/dtic/index.html>.
.

AFRL-RW-EG-TR-2012-092 HAS BEEN REVIEWED AND IS APPROVED FOR PUBLICATION IN ACCORDANCE WITH ASSIGNED DISTRIBUTION STATEMENT.

FOR THE DIRECTOR:

RUMMELT.NICHOLAS.I.1230474172 Digitally signed by RUMMELT.NICHOLAS.I.1230474172 DN: c=US, o=U.S. Government, ou=DoD, ou=PKI, ou=USAF, cn=RUMMELT.NICHOLAS.I.1230474172 Date: 2012.08.21 13:52:06 -05'00'

NICHOLAS I. RUMMELT
Acting Technical Advisor, RWW

RUTKOWSKI.ADAM.JAMES.1364263690 Digitally signed by RUTKOWSKI.ADAM.JAMES.1364263690 DN: c=US, o=U.S. Government, ou=DoD, ou=PKI, ou=USAF, cn=RUTKOWSKI.ADAM.JAMES.1364263690 Date: 2012.08.21 13:43:36 -05'00'

ADAM J. RUTKOWSKI
Program Manager

This report is published in the interest of scientific and technical information exchange, and its publication does not constitute the Government's approval or disapproval of its ideas or findings.

REPORT DOCUMENTATION PAGE

Form Approved
OMB No. 0704-0188

PLEASE DO NOT RETURN YOUR FORM TO THE ABOVE ADDRESS.

1. REPORT DATE *(DD-MM-YYYY)*	2. REPORT TYPE	3. DATES COVERED *(From - To)*
20-08-2012	Final	01-06-2010 - 23-07-2012

4. TITLE AND SUBTITLE

The Most Accurate Path from Point A to Point B is Not Necessarily a Straight Line

5a. CONTRACT NUMBER

5b. GRANT NUMBER

5c. PROGRAM ELEMENT NUMBER

62602F

6. AUTHOR(S)

Adam J Rutkowski

5d. PROJECT NUMBER

2068

5e. TASK NUMBER

82

5f. WORK UNIT NUMBER

10

7. PERFORMING ORGANIZATION NAME(S) AND ADDRESS(ES)

Air Force Research Laboratory
Munitions Directorate
101 W Eglin Blvd
Eglin AFB, FL 32542

8. PERFORMING ORGANIZATION REPORT NUMBER

AFRL-RW-EG-TR-2012-092

9. SPONSORING/MONITORING AGENCY NAME(S) AND ADDRESS(ES)

Air Force Research Laboratory
Munitions Directorate
101 W Eglin Blvd
Eglin AFB, FL 32542

10. SPONSOR/MONITOR'S ACRONYM(S)

AFRL/RW

11. SPONSOR/MONITOR'S REPORT NUMBER(S)

AFRL-RW-EG-TR-2012-092

12. DISTRIBUTION/AVAILABILITY STATEMENT

DISTRIBUTION A. Approved for public release; distribution unlimited. (96ABW-2012-0291)

13. SUPPLEMENTARY NOTES

DISTRIBUTION STATEMENT INDICATING AUTHORIZED ACCESS IS ON THE COVER PAGE AND BLOCK 12 OF THIS FORM. DATA RIGHTS RESTRICTIONS AND AVAILABILITY OF THIS REPORT ARE SHOWN ON THE NOTICE AND

14. ABSTRACT

This work studies the problem of guiding a vehicle from a known initial location to a known goal location as accurately as possible, without direct observation of the goal location (such as a bearing measurement, or line-of-sight to the goal), and without direct position measurements, such as those provided by GPS. The vehicle travels in a planar environment and has an onboard inertial measurement unit and an onboard visual system to measure bearing angles to features in the environment. Taking a zigzagging path toward the goal provides better position estimation than a straight path. For a given energy budget, there is a certain path width, or amplitude, that results in the best estimation performance, and this optimal path width depends on the sensor noise parameters. A batch estimator is derived to analyze the effect of the entire time history of the vehicle trajectory on final position estimation performance. The formulation results in a linear system of equations. The path width that minimizes the condition number of the system matrix also minimizes the final position estimation error when the feature bearing measurement noise is relatively large compared to the inertial measurement noise.

15. SUBJECT TERMS

vision-aided navigation; guidance; simultaneous localization and mapping

16. SECURITY CLASSIFICATION OF:			17. LIMITATION OF ABSTRACT	18. NUMBER OF PAGES	19a. NAME OF RESPONSIBLE PERSON
a. REPORT	b. ABSTRACT	c. THIS PAGE			Adam Rutkowski
UNCLAS	UNCLAS	UNCLAS	SAR	14	19b. TELEPHONE NUMBER *(Include area code)* 850-883-2632

Reset

Standard Form 298 (Rev. 8/98)
Prescribed by ANSI Std. Z39.18

List of Figures

The Most Accurate Path from Point A to Point B is Not Necessarily a Straight Line

Adam J. Rutkowski
Air Force Research Laboratory, Eglin AFB, FL, 32542, USA

Abstract

This work studies the problem of guiding a vehicle from a known initial location to a known goal location as accurately as possible, without direct observation of the goal location (such as a bearing measurement, or line-of-sight to the goal), and without direct position measurements, such as those provided by GPS. The vehicle travels in a planar environment and has an onboard inertial measurement unit and an onboard visual system to measure bearing angles to features in the environment. Taking a zigzagging path toward the goal provides better position estimation than a straight path. For a given energy budget, there is a certain path width, or amplitude, that results in the best estimation performance, and this optimal path width depends on the sensor noise parameters.

A batch estimator is derived to analyze the effect of the entire time history of the vehicle trajectory on final position estimation performance. The formulation results in a linear system of equations. The path width that minimizes the condition number of the system matrix also minimizes the final position estimation error when the feature bearing measurement noise is relatively large compared to the inertial measurement noise.

Nomenclature

a	acceleration
b	accelerometer bias
C_d	drag coefficient
J	estimation objective function
$\mathbf{x}$	position vector, $[x\ y]^T$
F	vehicle thrust, N
m	vehicle mass, kg
Δt	timestep length, s
β	inverse correlation time, 1/s
η	random disturbance
θ	bearing, degrees

Superscripts

i	timestep
k	feature number

Subscripts

f	feature
g	goal
v	vehicle

Accent symbols

$\hat{}$	estimated quantity
$\tilde{}$	measured quantity

This paper appeared in the Proceedings of the 2012 AIAA Guidance, Navigation, and Control Conference as paper number AIAA 2012-4761

1 Introduction

The objective of this work is to guide a vehicle from a known initial location to a known goal location as accurately as possible, without direct observation of the goal location (such as a bearing measurement, or line-of-sight to the goal), and without relying on a direct position measurement system such as the Global Positioning System (GPS). Several researchers have demonstrated that a visual system is an effective aid to an inertial navigation system when GPS is not available [4, 5]. Furthermore, it has been demonstrated that vehicle maneuvers can be used to improve position estimation accuracy. Bryson and Sukkarieh showed that flying an occasional orbit maneuver or s-turn improves both heading and vehicle position estimation accuracy [1]. Brink et al. demonstrated that estimation accuracy can be improved when a vehicle takes a continuously zigzagging path toward a goal [2]. In general, estimation accuracy improves as both the frequency and amplitude of the zigzagging path increase. However, paths with higher frequency and amplitude require more energy, and without a kinetic model of the vehicle (taking into consideration mass, drag, etc.), it is not possible to determine which combination of frequency and amplitude yield the best results for a given energy budget. Furthermore, the work of Brink et al. did not include a guidance law to direct the vehicle to the goal; rather, the vehicle made general progress along one Cartesian axis toward the goal.

Frew et. al have examined the problem of traveling from a known start location to a known goal location without position measurements [3]. They developed a control strategy based on minimizing an objective function that is the sum of four components - a control cost that limits control input, a navigation cost that moves the vehicle toward the goal, an uncertainty cost that moves the vehicle to improve knowledge of feature locations, and a safety cost that is used to avoid obstacles. However, they did not attempt to reach the goal as accurately as possible; rather, they attempted to reach the goal to within a specified distance, then return to the start location.

In this work, a guidance law is developed to maneuver a vehicle in a continuously zigzagging manner such that a constraint on the amount of energy (or, more accurately, impulse) expended by the vehicle is obeyed using a constant magnitude force over a specified time. In the final stage of the trajectory, a terminal guidance algorithm directs the vehicle to the goal. A batch estimator is also developed to examine the effect of the entire trajectory history on final position estimation accuracy.

2 Approach

For simplicity, the problem of traveling from a known initial location to a goal location without position feedback is considered in 2D, as shown in Figure 1. The vehicle has an onboard IMU and vision system. The IMU measures vehicle acceleration along the x and y axes, while the vision system measures the bearing angle to prominent visual features (e.g. SIFT features or Harris corners) in the environment. The vehicle orientation is constant and aligned with the global coordinate frame. The features are at initially unknown locations and are observed "on-the-fly". Since the position of the vehicle and the features must be determined, this is a simultaneous localization and mapping (SLAM) problem with the added requirement that the vehicle must reach a goal location as accurately as possible.

2.1 Kinetics

The vehicle kinetics are modeled using the decoupled set of equations in (1), where the drag force components, D_x and D_y, are proportional to the velocity components along their respective axes.

$$\begin{aligned} m\ddot{x}_v &= F_x - C_d\dot{x}_v \\ m\ddot{y}_v &= F_y - C_d\dot{y}_v \end{aligned} \tag{1}$$

The solution of the kinetics equation along the x-axis is given by (2), and the solution along the y-axis has the same form.

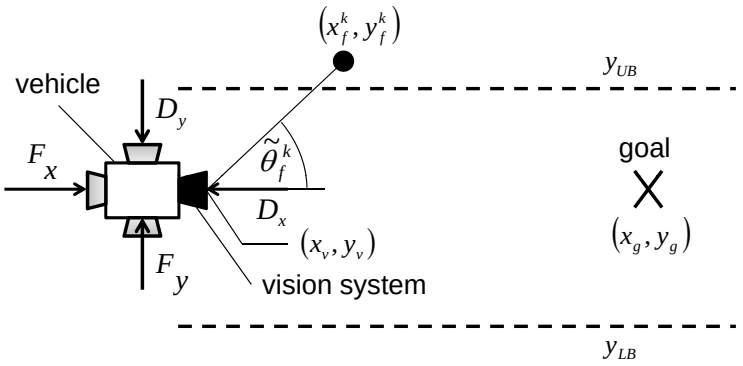

Figure 1: Problem scenario.

$$
\begin{aligned}
x_v^i &= x_v^{i-1} + \frac{F_x}{C_d}\Delta t + \left(\dot{x}_v^{i-1} - \frac{F_x}{C_d}\right)\frac{m}{C_d}\left(1 - \exp\left(-\frac{C_d}{m}\Delta t\right)\right) \\
\dot{x}_v^i &= \left(\dot{x}_v^{i-1} - \frac{F_x}{C_d}\right)\exp\left(-\frac{C_d \Delta t}{m}\right) + \frac{F_x}{C_d} \\
\ddot{x}_v^i &= -\frac{C_d}{m}\dot{x}_v^i + \frac{F_x}{m}
\end{aligned}
\tag{2}
$$

2.2 Sensing

The IMU model provides an acceleration measurement, $\tilde{a}$, that is the sum of the true acceleration, $\ddot{x}$, a Gaussian white noise component, η_a, and a bias component, b, as given by (3).

$$\tilde{a}^i = \ddot{x}^i + b^i + \eta_a^i \tag{3}$$

The bias follows a first order Gauss-Markov process described by (4) and (5), where the Gaussian white noise term $\eta_{\Delta b}$ has a standard deviation of $\sigma_{\Delta b}$, and over time, the bias will have a standard deviation of σ_b.

$$\sigma_{\Delta b} = (1 - \exp(-2\beta_a \Delta t))^{0.5}\sigma_b \tag{4}$$

$$b^i = \exp(-\beta_a \Delta t) b^{i-1} + \eta_{\Delta b}^i \tag{5}$$

The visual system model is omnidirectional and capable of identifying features at an infinite distance. The feature bearing measurement is computed according to (6), where $\text{atan}(y, x)$ is the 4 quadrant inverse tangent, and the bearing measurement noise, η_θ, is zero-mean Gaussian with a standard deviation σ_θ.

$$\tilde{\theta} = \text{atan}(y_f - y_v, x_f - x_v) + \eta_\theta \tag{6}$$

2.3 Estimation

Since the estimation performance depends on the entire trajectory history, a batch estimator is used to solve for all states at all points in time. A batch estimator was chosen instead of a recursive estimator, such as an Extended Kalman Filter (EKF), with the hope to gain insight into how the entire time history of the trajectory influences the estimation performance. Furthermore, the batch estimator does not require a delayed feature initialization scheme that is commonly used with an EKF [1].

The state vector is arranged according to (7), where $\hat{\mathbf{x}}_f = [x_f^1 \ y_f^1 \ ... \ x_f^{N_f} \ y_f^{N_f}]^T$, $\hat{\mathbf{b}} = [b_x \ b_y]^T$, and $\hat{\mathbf{x}}_v = [x_v^1 \ y_v^1 \ ... \ x_v^N \ y_v^N]^T$ for N total timesteps and N_f total features.

$$\hat{\mathbf{x}} = [\hat{\mathbf{x}}_f^T \ \ \hat{\mathbf{b}}^T \ \ \hat{\mathbf{x}}_v^T]^T \tag{7}$$

Notice that although the accelerometer bias is modeled as a first order Gauss-Markov process (as in (5)), the accelerometer bias is treated as constant in the state vector. This is done to simplify the estimation procedure and reduce the dimension of the resulting equations.

The state vector is estimated by minimizing an estimation objective function (8) that consists of two parts, a feature bearing estimation error, J_f, defined in (9), and an acceleration error, J_a, defined in (10).

$$J = \sum_{i=1}^{n} \sum_{k=1}^{n_f} w^{i,k} J_f(t_i, k) + \lambda \sum_{i=2}^{n-1} J_a(t_i) \tag{8}$$

$$J_f(t_i, k) = \left(\left(\hat{x}_v^i - \hat{x}_f^k \right) \sin \tilde{\theta}_f^{i,k} - \left(\hat{y}_v^i - \hat{y}_f^k \right) \cos \tilde{\theta}_f^{i,k} \right)^2 \tag{9}$$

$$J_a(t_i) = \left(\hat{\ddot{x}}_v^i - (\tilde{a}_x^i - \hat{b}_x^i) \right)^2 + \left(\hat{\ddot{y}}_v^i - (\tilde{a}_y^i - \hat{b}_y^i) \right)^2 \tag{10}$$

The feature bearing objective function of (9) is derived from the fact that in the ideal case, $\tan(\theta) = \sin(\theta)/\cos(\theta) = (y_f - y_v)/(x_f - x_v)$. At a given moment in time, multiplying J_f by weighting terms $w^{i,k}$ and summing over all features leads to an objective function that is the basis of the classic Stansfield estimator [6]. If the weighting terms, $w^{i,k}$, are chosen appropriately, the Stansfield estimator provides an elegant approximation to the maximum likelihood estimator for vehicle position when the feature locations are known. However, for the current problem, the features are in unknown locations. This is where the acceleration error term comes in. The acceleration objective function describes the disagreement between the acceleration measurements and estimates, and the term λ describes the relative importance between acceleration errors and bearing errors.

The estimated acceleration is derived directly from the estimated position using the central difference scheme of (11).

$$\hat{\ddot{x}}_v^i = \frac{\hat{x}_v^{i+1} - 2\hat{x}_v^i + \hat{x}_v^{i-1}}{(\Delta t)^2} \tag{11}$$

The state estimate is determined by setting the derivative of J with respect to $\hat{\mathbf{x}}$ to zero. This leads to the following linear system, where the system matrix $\mathbf{L}$ depends only on the feature bearing measurements, and the vector $\mathbf{R}$ depends only on the accelerometer measurements.

$$\mathbf{L}\hat{\mathbf{x}} = \mathbf{R} \tag{12}$$

The equation (12) is solved twice, once with the weights $w^{i,k}$ set to one for all features at all points in time, then again with the weights proportional to the inverse of the square of the estimated range from the first solution. The improvement in estimation accuracy that results by adjusting the weights in this manner and solving (12) a second time will be demonstrated in the results section.

In the matrix $\mathbf{L}$, there are several terms involving $\sin^2(\theta)$, $\cos^2(\theta)$, and $\sin(\theta)\cos(\theta)$. If these terms are computed directly from the bearing measurements, the noise in $\tilde{\theta}$ will cause these terms to be biased from their expected values. This will in turn cause the vehicle and feature position estimates to be biased, as will be shown in the results section. This can be fixed if one knows the magnitude of the noise in $\tilde{\theta}$, which can be determined from a calibration procedure of the bearings measurement device. The corrections in (13) are based on approximating $\sin(\eta_\theta) \approx \eta_\theta$ and $\cos(\eta_\theta) \approx 1 - \eta_\theta^2$.

$$\begin{aligned}
\sin^2(\theta) &\approx \frac{(1 - \sigma_\theta^2)\sin^2(\tilde{\theta}) - \sigma_\theta^2 \cos^2(\tilde{\theta})}{1 - 2\sigma_\theta^2} \\
\cos^2(\theta) &\approx \frac{(1 - \sigma_\theta^2)\cos^2(\tilde{\theta}) - \sigma_\theta^2 \sin^2(\tilde{\theta})}{1 - 2\sigma_\theta^2} \\
\sin(\theta)\cos(\theta) &\approx \frac{\sin(\tilde{\theta})\cos(\tilde{\theta})}{1 - 2\sigma_\theta^2}
\end{aligned} \tag{13}$$

2.4 Guidance

2.4.1 Midcourse

A natural way to achieve the excitation necessary for observability of the states is to simply let the vehicle zigzag toward the goal. To achieve this behavior, the vehicle exerts a constant thrust along the x-axis, F_x, and switches the sign of the constant magnitude lateral force, F_y, whenever the vehicle moves from a location between two parallel boundaries to a location outside the boundaries. These boundaries are labeled as y_{LB} and y_{UB} in Figure 1, where $y_{UB} = y_{BO} + y_B$ and $y_{LB} = y_{BO} - y_B$.

2.4.2 Terminal

After a certain amount of time, the vehicle is directed to a prespecified goal location using Algorithm 1. For this work, only the y-coordinate of the goal location, y_g, is specified. At a given time $t^i < t^N$, y^* is the position along the y-axis that the vehicle would reach at time t^N if $F_y = -F_{ymag}\,\text{sign}(y - y_g)$, and the time-to-go $t_{go} = t^N - t^i$. During midcourse, when y^* gets close to y_g, this is the point when F_y must point toward the goal, otherwise, the vehicle would never reach the goal. The points y^{**} and y^{***} are also checked when the condition specified by y^* alone does not allow sufficient time to reach the goal. Expressions for y^*, y^{**} and y^{***} are given in (14)–(16).

Algorithm 1 Terminal Guidance

if $(|y^i| > 0.99y^*)$ **then**
  $F_y^i = -F_{ymag}\,\text{sign}(y^i)$
else if $(y^{**} > y_g$ and $y_v^i < y_g$ and $\dot{y}^i > 0)$ **then**
  $F_y^i = -F_{ymag}$
else if $(y^{***} < y_g$ and $y_v^i > y_g$ and $\dot{y}^i < 0)$ **then**
  $F_y^i = F_{ymag}$
end if

$$y^* = \frac{F_y}{C_d} t_{go} + \left(-\dot{y}^i\,\text{sign}(y^i) - \frac{F_y}{C_d} \right) \frac{m}{C_d} \left(1 - \exp\left(-\frac{C_d t_{go}}{m} \right) \right) \tag{14}$$

$$y^{**} = -\frac{F_y}{C_d} t_{go} + \left(\dot{y}^i + \frac{F_y}{C_d} \right) \frac{m}{C_d} \left(1 - \exp\left(-\frac{C_d t_{go}}{m} \right) \right) + y^i \tag{15}$$

$$y^{***} = \frac{F_y}{C_d} t_{go} + \left(\dot{y}^i - \frac{F_y}{C_d} \right) \frac{m}{C_d} \left(1 - \exp\left(-\frac{C_d t_{go}}{m} \right) \right) + y^i \tag{16}$$

The meaning of y^{**} and y^{***} is apparent in Figure 2. Near the point $x_v = 70$, with no terminal guidance, F_y is positive and remains so until the vehicle reaches the upper bound $y_{UB} = 3$. However, the vehicle does not reach the goal. Using only y^* guidance, the sign of F_y switches to negative at the point when y_v becomes positive, but this thrust cannot overcome the momentum of the vehicle to force it back to the goal location in time. Using the full terminal guidance law, y^{**} becomes $> y_g$ when y_v is still $< y_g$, thus from Algorithm 1, the sign of F_y switches to negative just in time for the vehicle to reach y_g at t^N.

3 Results

In the first test scenario, there are two rows of feature points, one row of feature points located at $y = 15$ and the other at $y = -15$. The features are equally spaced along each row with a spacing of 15 m. The vehicle travels for 150 seconds, and the bearings sensor and inertial sensor take measurements at 10 Hz.

The resulting trajectory estimate when $y_B = 5$ is shown in Figure 3. The mean final position estimation error is 0.16 m over 1000 Monte Carlo runs. In comparison, the dead-reckoned final position estimate using only IMU data sampled at 100 Hz with perfect bias initialization had a mean error of 33.85 m as computed from 1000 Monte Carlo runs.

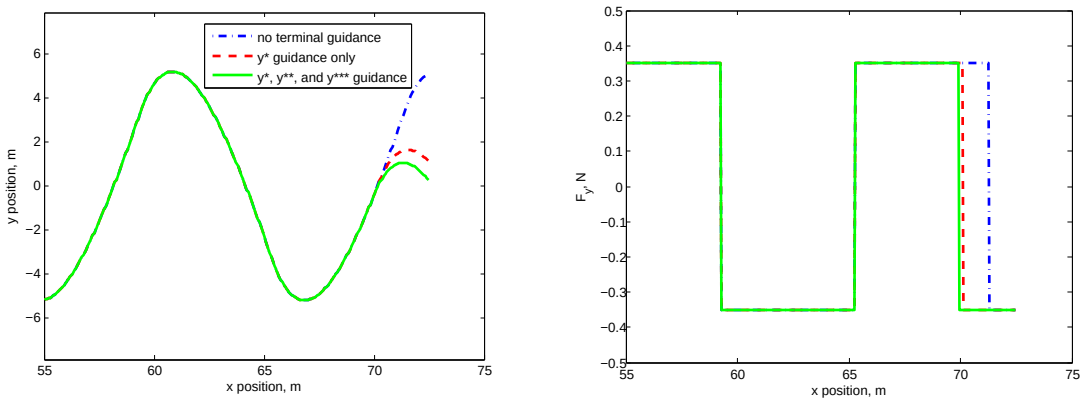

Figure 2: (left) Effect of terminal guidance on trajectory. The goal location has $y_g = 0$. (right) Applied lateral force.

For one of the Monte Carlo runs, the true and estimated accelerometer bias are also plotted in Figure 3. The estimated components (4.93×10^{-3}, 1.588×10^{-2}) of the accelerometer bias are nearly equal to the mean of the true bias components (5.29×10^{-3}, 1.595×10^{-2}), which is the best one can hope for when approximating a varying quantity as a constant.

It is clear from Figure 3 that the corrections given in (13) are necessary to avoid a biased final position estimate. Furthermore, solving (12) twice, where the weights for the second solution are based on the first solution, produces a lower mean final position error than the first solution (0.16 m vs. 0.23 m). The weights could be adjusted again based on the second solution of (12), then (12) could be solved a third time with the hope of obtaining an even more accurate solution. However, for this particular scenario, no improvement was obtained by solving (12) a third time.

The mean final position error for different values of y_B and two different values for the standard deviation of the bearings sensor measurement noise is shown in Figure 3. In general, it appears that there is an optimal spacing between the bounds that results in the best estimation performance, and this optimal spacing tends to be lower for lower values of σ_θ. The exact and approximate values of the condition number, computed using cond and condest in Matlab, are also shown in Figure 3. Notice that the condition number and the mean final position error are both minimized at nearly the same value of y_B when $\sigma_\theta = 1^o$. However, when $\sigma_\theta = .3^o$, the noise in the bearing measurements becomes less important compared to the noise in the IMU measurements. Since the vector $\mathbf{R}$ depends on the IMU measurements, and the condition number indicates the sensitivity of the solution of (12) to changes only in $\mathbf{L}$ (and thus noise in the bearing measurements), the condition number of $\mathbf{L}$ is not a good indicator of system performance when the bearing measurement noise is relatively small compared to the inertial measurement noise.

The batch estimation procedure may seem like a computationally expensive approach, but the linear system given in (12) can actually be solved quickly due to the sparsity of $\mathbf{L}$. For this particular scenario, $\mathbf{L}$ is a 3024×3024 sparse matrix, and the solution of (12) is obtained in 0.012 seconds in Matlab®on an Intel®Xeon®W3550 CPU. Recall that (12) is solved twice to obtain the estimate, first with the weights $w^{i,k}$ set to one, then again with the weights proportional to the inverse of the square of the estimated feature ranges. When the overhead required to form $\mathbf{L}$ and $\mathbf{R}$ is taken into account, each trajectory solution in our implementation requires about 0.05 seconds to compute for this scenario.

In the second test scenario, there is only one row of feature points located at $y = 15$. Figure 4 shows the mean estimation error for different values of y_B and y_{BO}. The trajectory is also shown when $y_B = 5$ and $y_{BO} = 15$. Notice that when y_{BO} is closer to the feature points, the bounds do not need to be as far apart to achieve a desirable estimation accuracy. Also, in contrast to the previous scenario, the estimation error does not tend to increase as quickly with increasing bound separation.

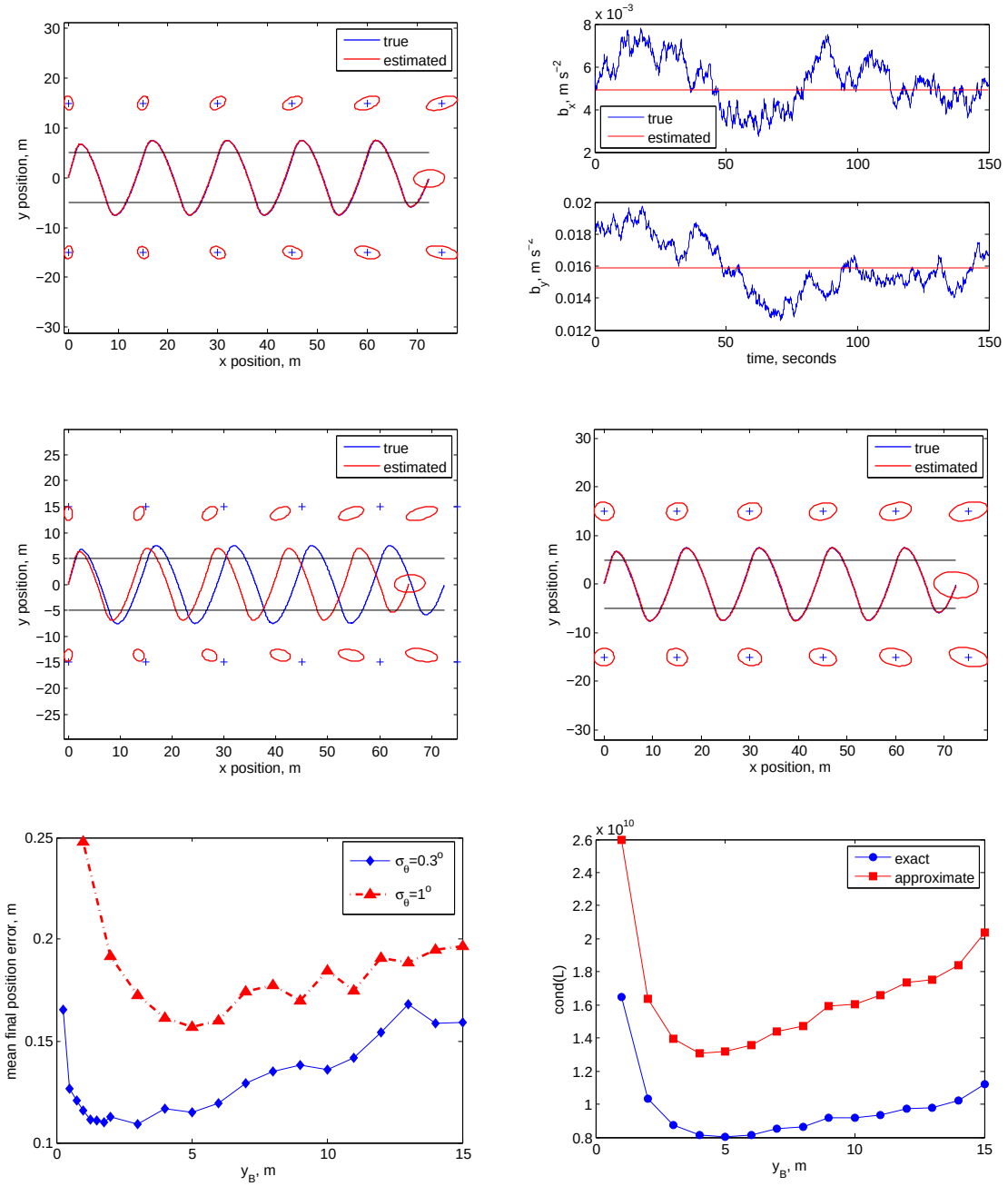

Figure 3: (top left) The true vehicle trajectory is shown for $y_B = 5$ and $\sigma_\theta = 1^o$, along with an estimate of the trajectory from one of the 1000 Monte Carlo runs and a 20σ covariance ellipse on the final position estimate for all Monte Carlo runs. The mean estimation error in final position in this case is 0.16 m. The true feature locations are marked with '+' symbols, and the 20σ covariance ellipses for the feature locations are also shown. The bounds y_{UB} and y_{LB} are marked by parallel lines. (top right) The true accelerometer bias and its estimate are plotted over time. (middle left) Trajectory estimation results with $y_B = 5$ and $\sigma_\theta = 1^o$ without applying the corrections of (13), the covariance is roughly the same, but the final position estimate is biased by -6.67 m along the x-axis. (middle right) If the estimator is run only once without re-weighting based on estimated feature distance, the mean estimation error in final position increases to 0.23 m. (bottom left) The mean position error, computed from 1000 Monte Carlo simulations for $1 \leq y_B \leq 15$ is shown for two different levels of feature bearing noise. (bottom right) The exact and approximate condition numbers of the matrix $\mathbf{L}$ as respectively computed with cond and condest in Matlab®are shown for various values of y_B.

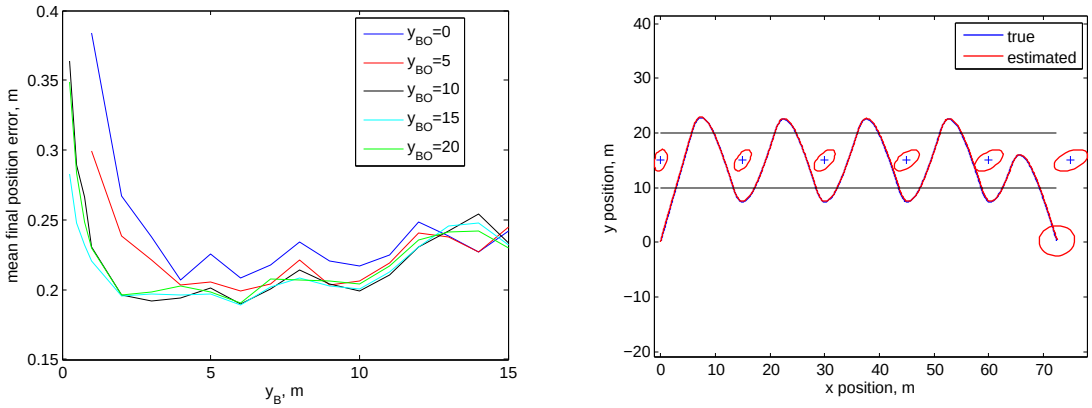

Figure 4: (left) The mean position error is shown for various values of y_B and y_{BO} in the second test scenario (described in the text). (right) The trajectory when $y_B = 5$ and $y_{BO} = 15$

4 Conclusions and Future Work

In this work, a batch estimator for vision-aided inertial navigation was developed and used to study the problem of traveling from a known location to a goal location without position feedback. A guidance law was developed to excite the motion of the vehicle to improve observability of the vehicle states. For a given energy budget, there is a certain path width, or amplitude, that results in the best estimation performance, and this optimal path width, as defined by the parameter y_B, depends on the sensor noise parameters. The formulation of the batch estimator results in a linear system of equations. The path width that minimizes the condition number of the system matrix also minimizes the final position estimation error when the feature bearing measurement noise is relatively large compared to the inertial measurement noise. However, if the feature bearing measurement noise is relatively small, the condition number of the system matrix is not a good indicator of the final position estimation error.

Although the batch estimator developed in this work can be used as an analysis tool for determining the optimal path width that results in minimum final position error, it does not yet help in developing heuristic rules for determining an optimal flight path while in flight. It is only useful in finding the optimal path width given all the measurements up to the goal location, yet the measurements of course are not known *a priori*. For future work, the condition number of the batch estimator may be used to discover paths that produce even better estimation performance than the class of trajectories explored in this work. Analysis of the information provided by the measurements during these trajectories may then be used to develop rules for trajectory planning that can be implemented in real time.

Acknowledgments

I thank Dr. Fariba Fahroo at the Air Force Office of Scientific Research for providing support for this work. Also, I thank Dr. Kevin Brink, Mr. Peter Lommel, and Dr. Paul Debitetto for spirited discussions regarding the merits of the batch estimator developed in this paper, and Dr. Brink for reviewing a draft of this manuscript.

References

[1] Bryson M, Sukkarieh S (2008) Observability analysis and active control for airborne SLAM. IEEE transactions on aerospace and electronic systems 44(1), 261-280.

[2] Brink K, Hurtado J, Soloviev A, Rutkowski A, Klausutis T (2010) Integrated estimation and control approach for vision aided inertial navigation. In: Proceedings of the AIAA Infotech@Aerospace Conference, pp 1–11.

[3] Frew EW, Langelaan J, Joo S (2006) Adaptive receding horizon control for vision-based navigation of smal unmanned aircraft. Proceedings of the 2006 American Control Conference, 2160-2165.

[4] Jones ES, Soatto S (2011) Visual-inertial navigation, mapping and localization: a scalable real-time causal approach. Interntaional Journal of Robotics Research 30(4), 405-430.

[5] Mourikis AI, Roumeliotis SI (2007). A multi-state constraint Kalman filter for vision-aided inertial navigation. In: Proceedings of the IEEE International Conference on Robotics and Automation, pp 3565-3572.

[6] Stansfield RG (1947) Statistical theory of d.f. fixing. J of IEE - Part IIIA 94(15), 762-770.

DISTRIBUTION LIST
AFRL-RW-EG-TR-2012-092

DEFENSE TECHNICAL INFORMATION CENTER - 1 Electronic Copy (1 file &1 format)
ATTN: DTIC-OCA (ACQUISITION)
8725 JOHN J. KINGMAN ROAD, SUITE 0944
FT. BELVOIR VA 22060-6218

AFRL/RWOC (STINFO Office)	- 1 Hard (color) Copy
AFRL/RW CA-N	- STINFO Officer to provide notice of publication